This Supplemental Information file includes:

SUPPLEMENTAL FIGURES

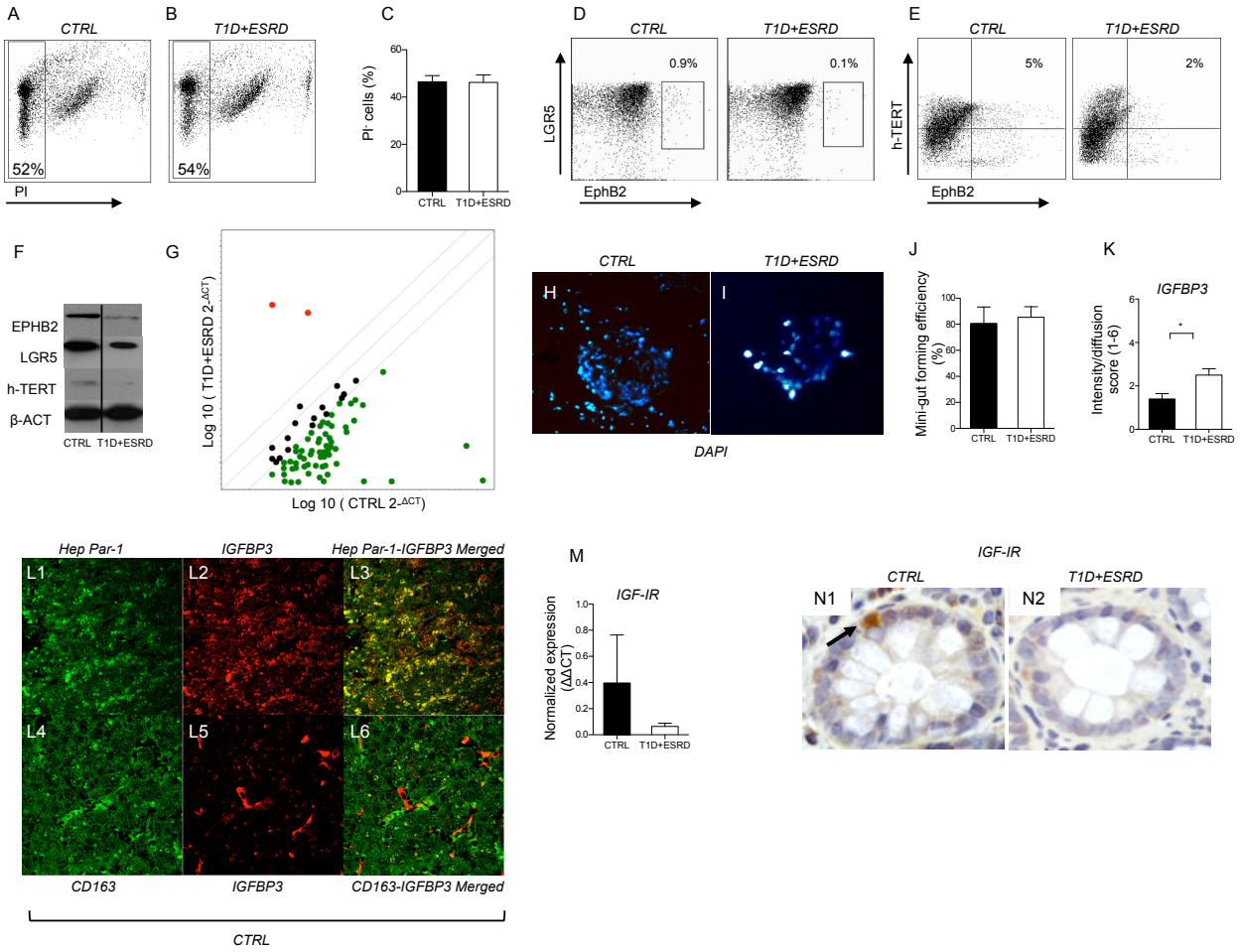

Figure S1. CoSC profile, *in vitro* generation of mini-guts, expression of IGFBP3 in the liver and of IGF-IR on CoSCs in long-standing T1D and healthy subjects. Related to Figure 2.

A, B. Representative flow dot plots of PI^- cell gating strategy in healthy subjects (CTRL) and long-standing T1D individuals (T1D+ESRD). **C**. Bar graphs depict results of flow cytometric analysis of PI^- cells in freshly isolated crypts (n=10 CTRL and n=10 T1D+ESRD). **D-E**. Representative flow dot plots of $EphB2^{hi}LGR5^+$ (D) and $EphB2^+h\text{-}TERT^+$ (E) cells in healthy subjects (CTRL) and long-standing T1D individuals (T1D+ESRD). **F**. Western blot analysis (cropped blots) confirms low expression of EphB2, LGR5, h-TERT in *in vitro* isolated intestinal crypts of long-standing T1D individuals (T1D+ESRD). Full-length blots are presented in Fig. 5.

n=5 subjects per group were evaluated. **G**. Scatter plot representing the stem cell transcriptome profiling examined in freshly isolated intestinal crypts of healthy subjects (CTRL) and long-standing T1D individuals (T1D+ESRD). n=10 subjects per group. **H-I**. Representative images of freshly isolated crypts obtained from healthy subjects and long-standing T1D individuals stained with DAPI. 20X magnification. **J**. Bar graph representing percentage of mini-guts forming efficiency of plated crypts obtained from healthy subjects and long-standing T1D individuals at 12 hours. n=10 subjects per group. **K**. Bar graph representing the calculated combined score of IGFBP3 intensity/diffusion (0-6) upon immunohistochemical evaluation in liver samples obtained from healthy subjects and long-standing T1D individuals. n=3 subjects per group. **L1-L6**. Representative images (63X magnification) of IGFBP3 expression in the liver. Immunofluorescence confirmed the colocalization of Hep Par-1^+ cells and IGFBP3 expression (L1-L3), while no colocalization was observed between IGFBP3 and $CD163^+$ cells (L4-L6). **M**. Bar graph depicts normalized mRNA expression of the IGF-I receptor (IGF-IR) measured by quantitative RT-PCR on isolated intestinal crypts. All samples were run in triplicate and normalized to the housekeeping gene ACTB using the ΔΔCt method. **N1-N2**. Representative pictures of IGF-IR^+ cells on rectal mucosa samples obtained from CTRL and from T1D+ESRD individuals. Black arrow indicates positive cells at the crypt base. 400X magnification. Data are expressed as mean ± standard error of the mean (SEM) unless differently reported. $^*p<0.01$.

Abbreviations: PI, propidium iodide; IGF-I, insulin-like growth factor 1; IGFBP3, insulin-like growth factor binding protein 3; IGF-IR, insulin-like growth factor 1 receptor; CoSC, colonic stem cell; T1D, type 1 diabetes; ESRD, end-stage renal disease; CTRL, healthy subjects; EphB2, Ephrin B receptor 2; LGR5, leucine-rich repeat containing G protein-coupled receptor 5; RT-PCR, real-time polymerase chain reaction; ACTB, beta actin; SEM, standard error of the mean.

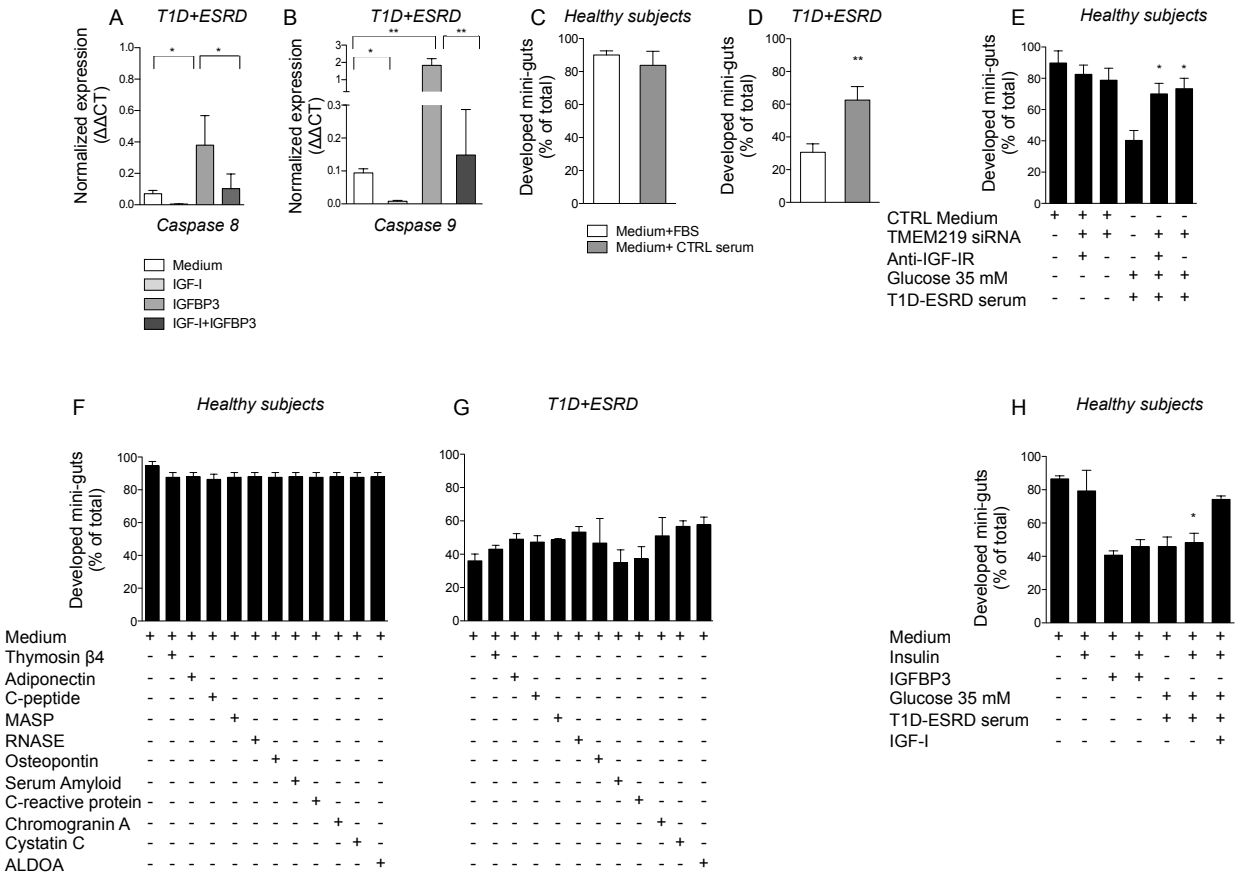

Figure S2. **Caspase expression in IGF-I/IGFBP3 cultured mini-guts and the lack of effect of other circulating factors found in our serum proteomic analysis. Related to Figure 3**.

A. Bar graph representing normalized mRNA expression of Caspase 8 in crypts isolated from individuals with T1D+ESRD cultured in the presence of IGFBP3, IGF-I+IGFBP3 and IGF-I, performed in triplicate. **B**. Bar graph representing normalized mRNA expression of Caspase 9 in crypts isolated from individuals with T1D+ESRD cultured in the presence of IGFBP3, IGF-I+IGFBP3 and IGF-I, performed in triplicate**. C, D**. Bar graph grouping percentage of mini-guts developed from healthy subjects (C) and from long-standing T1D individuals (D), cultured in the presence of medium with FBS and medium with serum obtained from healthy subjects, "CTRL serum". Assay was performed in triplicate. **E**. Bar graph grouping percentage of developed mini-guts of the total obtained from healthy subjects, cultured for 8 days, exposed to siRNA targeting

TMEM219 and anti-IGF-IR, and finally compared to TMEM219-expressing crypts in medium alone and in medium+high glucose+long-standing T1D serum. Assay was performed in triplicate. **F, G**. Bar graph grouping percentage of developed mini-guts at 8 days of culture, obtained from healthy subjects (F) and long-standing T1D individuals (G) cultured in the presence of medium alone and various molecules identified by proteomic analysis (Table S5). Assay was performed in triplicate. **H**. Bar graph grouping percentage of mini-guts obtained from healthy subjects and cultured in the presence of medium alone, medium+high glucose, medium+high glucose and long-standing T1D serum, IGF-I, IGFBP3 with/without insulin. Assay was performed in triplicate. Data are expressed as mean ± standard error of the mean (SEM) unless differently reported. $^{*}p<0.01$; $^{**}p<0.001$.

Abbreviations: IGF-I, insulin-like growth factor 1; IGFBP3, insulin-like growth factor binding protein 3; IGF-IR, insulin-like growth factor 1 receptor; CoSC, colonic stem cell; T1D, type 1 diabetes; ESRD, end-stage renal disease; CTRL, healthy subjects; RT-PCR, real-time polymerase chain reaction; ACTB, beta actin; SEM, standard error of the mean; siRNA, small RNA interference; ALDOA, fructose-bisphosphate aldolase A; RNASE, pancreatic ribonuclease; MASP, mannan-binding lectin serine protease 1.

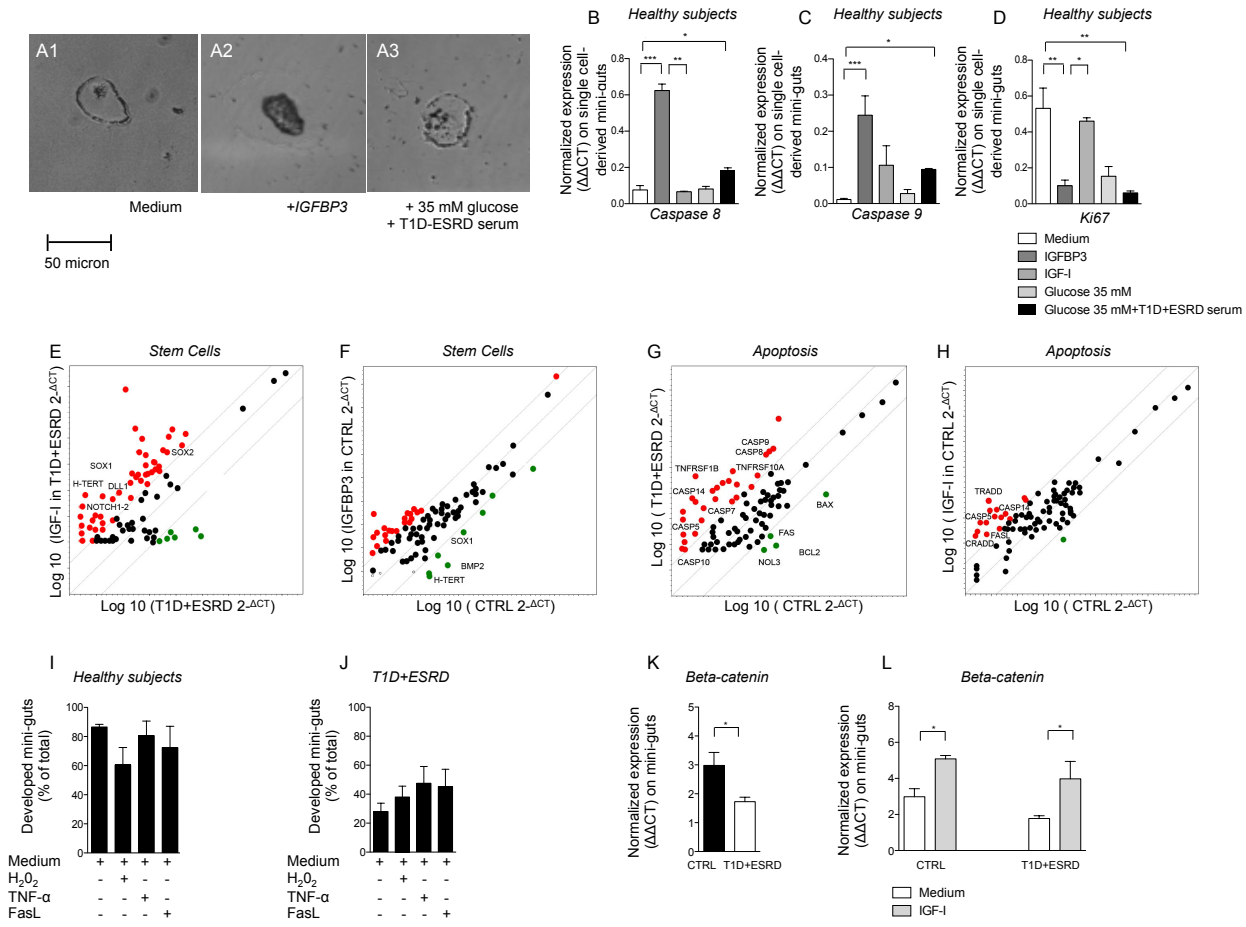

Figure S3. **Effect of IGF-I/IGFBP3 dyad on single cell-derived mini-guts, on stem cell transcriptome profile and on apoptotic pathways. Related to Figure 4**.

A1-A3. Representative images of single cell-derived mini-guts, cultured for 8 days *in vitro* obtained from previously isolated EphB2^{+} sorted cells of healthy subjects and cultured with medium alone, medium+IGFBP3, medium+glucose 35 mM+long-standing T1D serum. Images are shown at 10X magnification. Scale bar 50 micron. **B**, **C**, **D**. Bar graph representing normalized mRNA expression of Caspase 8, Caspase 9 and Ki67 in single cell-derived mini-guts grown from flow-sorted EphB2^{+} cells isolated from healthy subjects and cultured in different conditions. Assay was performed in triplicate**. E, F**. Scatterplot representing the stem cell transcriptome profiling examined in freshly isolated intestinal crypts of healthy subjects (CTRL) and long-standing T1D individuals (T1D+ESRD) cultured with/without IGFBP3 and IGF-I.

Assays were performed in triplicate. **G, H**. Scatterplot representing the apoptosis transcriptome profiling examined in freshly isolated intestinal crypts of healthy subjects (CTRL) and long-standing T1D individuals (T1D+ESRD) cultured with/without IGF-I. A table summarizes genes and pathways analyzed (Table S3). Assays were performed in triplicate. **I, J**. Bar graph grouping percentage of mini-guts developed from crypts obtained from healthy subjects (I) and long-standing T1D (J) and then cultured in the presence of medium alone, Fas ligand (FasL), hydrogen peroxide (H_2O_2) and tumor necrosis factor alpha (TNF-α). Assay was performed in triplicate. **K, L**. Bar graphs representing normalized mRNA expression of beta-catenin in mini-guts generated from crypts isolated from healthy subjects and individuals with T1D+ESRD (K) and cultured in the presence of IGF-I performed in triplicate (L). Data are expressed as mean ± standard error of the mean (SEM) unless differently reported. $^{*}p<0.01$; $^{**}p<0.001$; $^{***}p<0.0001$.

Abbreviations: IGF-I, insulin-like growth factor 1; IGFBP3, insulin-like growth factor binding protein 3; T1D, type 1 diabetes; ESRD, end-stage renal disease; CTRL, healthy subjects; RT-PCR, real-time polymerase chain reaction; ACTB, beta actin; SEM, standard error of the mean; FasL, Fas ligand; H_2O_2, hydrogen peroxide; TNF-α, tumor necrosis factor alpha.

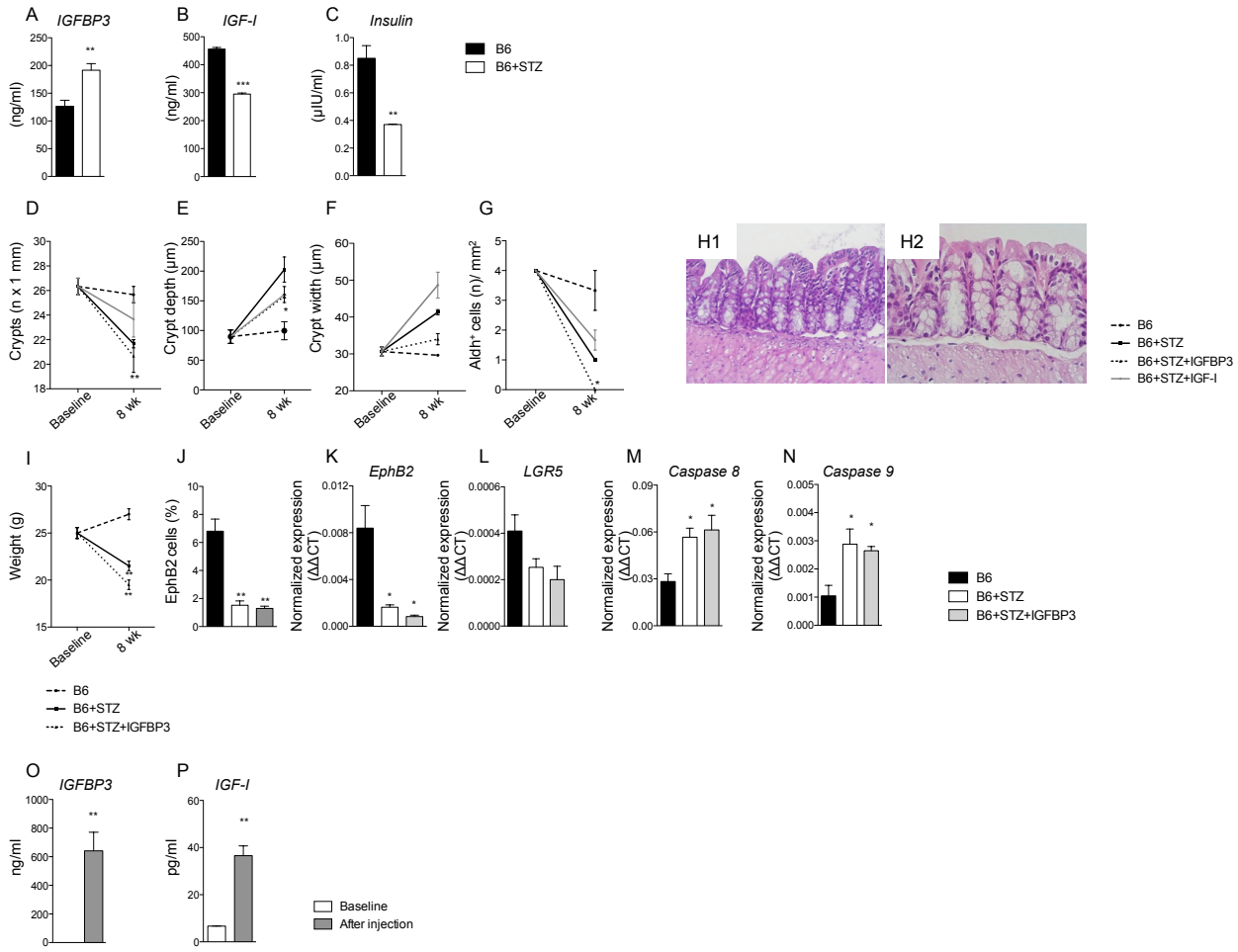

Figure S4. **Manipulating IGF-I/IGFBP3 dyad in preclinical models of diabetic enteropathy**. **Related to Figure 4**.

A. Bar graph representing murine IGFPB3 circulating levels measured in naïve B6 mice (B6) and STZ-treated B6 mice (B6+STZ). **B**. Bar graph representing murine IGF-I circulating levels measured in naïve B6 mice (B6) and STZ-treated B6 mice (B6+STZ). **C**. Bar graph representing insulin serum levels measured in naïve B6 mice (B6) and STZ-treated B6 mice (B6+STZ). **D**, **E**, **F**. Line graphs report the number of crypts (D), depth of crypts (E) and width of crypts (F) assessed on intestinal lower tract sections harvested at baseline and after 8 weeks from naïve B6 (B6), STZ-treated B6 mice developing diabetic enteropathy (B6+STZ) and STZ-B6 mice treated with IGFBP3 (B6+STZ+IGFBP3) or with IGF-I (B6+STZ+IGF-I). n=3 mice per group. **G**. Line

graph represents the number of $Aldh^+$ cells/mm^2 in immunostained sections of B6, STZ-treated B6 mice developing diabetic enteropathy and STZ-B6 mice treated with IGFBP3 (B6+STZ+IGFBP3) or with IGF-I (B6+STZ+IGF-I). **H1-H2**. Representative images of intestinal crypts on H&E sections of STZ-B6 mice treated with IGFBP3 (B6+STZ+IGFBP3), (H1) or with IGF-I (B6+STZ+IGF-I), (H2). Histology magnification, 400X. **I**. Line graph reporting the weight of naïve B6 (B6), STZ-treated B6 mice developing diabetic enteropathy (B6+STZ) and STZ-treated B6 mice developing diabetic enteropathy treated with IGFBP3 (B6+STZ+IGFBP3). n=3 mice per group. **J**. Bar graph representing results of flow cytometric analysis of $EphB2^+$ cells in intestinal samples collected from naïve B6 mice (B6), STZ-treated B6 mice and in STZ-B6 mice treated with IGFBP3 (B6+STZ+IGFBP3). **K, L**. Bar graph representing normalized mRNA expression of EphB2 (K) and LGR5 (L) in intestinal samples collected from naïve B6 mice (B6), STZ-treated B6 mice and in STZ-B6 mice treated with IGFBP3 (B6+STZ+IGFBP3). **M, N**. Bar graph representing normalized mRNA expression of Caspase 8 (M) and Caspase 9 (N) in intestinal samples collected from naïve B6 mice (B6), STZ-treated B6 mice and in STZ-B6 mice treated with IGFBP3 (B6+STZ+IGFBP3). **O**, **P**. Bar graphs representing peripheral levels of human IGFBP3 and human IGF-I before and after 1 hour from injection in B6 mice. Data are expressed as mean ± standard error of the mean (SEM) unless differently reported. $^{*}p<0.01$; $^{**}p<0.001$; $^{***}p<0.0001$.

Abbreviations: STZ, streptozoticin-treated; B6, C57BL/6J mice; IGF-I, insulin-like growth factor 1; IGFBP3, insulin-like growth factor binding protein 3; H&E, hematoxylin and eosin; EphB2, Ephrin B receptor 2; LGR5, leucine-rich repeat containing G protein-coupled receptor 5; Aldh, Aldehyde dehydrogenase; SEM, standard error of the mean.

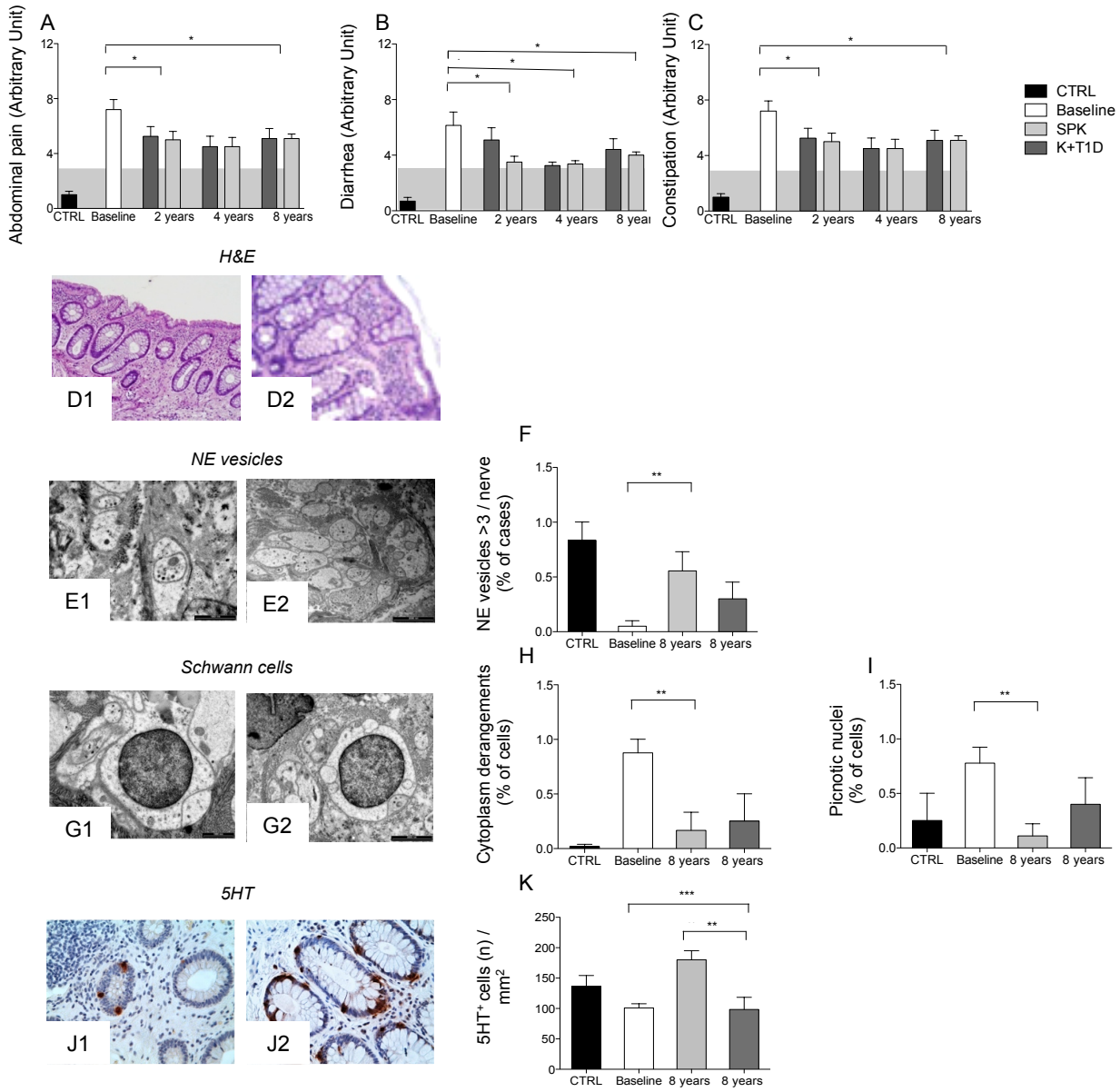

Figure S5. The treatment of long-standing T1D with SPK ameliorates diabetic enteropathy. Related to Figure 4 and 5.

A, B, C. Bar graphs depict the score of abdominal pain, diarrhea and constipation according to the GSRS questionnaire in healthy subjects (CTRL), long-standing T1D individuals (Baseline), T1D+ESRD who underwent kidney pancreas (SPK) or kidney alone (K+T1D) transplantation. Gray area indicates normal range for all the parameters. Statistics are expressed as mean ± SEM.

D1-D2, E1-E2, G1-G2, J1-J2. Representative pictures of H&E staining and ultrastructural analysis of neural structures, Schwann cells, and $5HT^+$ cells performed on rectal mucosa biopsy samples obtained from T1D+ESRD who underwent kidney pancreas (SPK) or kidney alone (K+T1D) transplantation at 8 years of follow-up. 400X magnification. **F, H, I, K**. Bar graphs report the measurements of neuroendocrine vesicles (percentage of cases with >3 NE vesicles detected per nerve terminal), percentage of Schwann cells with picnotic nuclei and cytoplasm derangements (percentage of positive cases) using electron microscopy, $5HT^+$ cells, performed on bioptic samples obtained from rectal mucosa of CTRL, long-standing T1D individuals (Baseline), T1D+ESRD who underwent kidney pancreas (SPK) or kidney alone (K+T1D) over an 8-year follow-up period. Statistics are expressed as mean ± SEM. n=20 CTRL, n=30 SPK, n=30 K+T1D and n=60 T1D+ESRD subjects were evaluated. All parameters examined were statistically significantly different when comparing different groups as following: $^{*}p<0.01$; $^{**}p<0.001$; $^{***}p<0.0001$.

Abbreviations: GSRS, Gastrointestinal Symptom Rating Scale; SPK, simultaneous kidney-pancreas transplantation; K+T1D, kidney transplantation alone in type 1 diabetes; CTRL, healthy subjects; T1D, type 1 diabetes; ESRD, end-stage renal disease; 5HT, serotonin; H&E, hematoxylin and eosin; NGF, neural growth factor; SEM, standard error of the mean; NE, neuroendocrine vesicles.

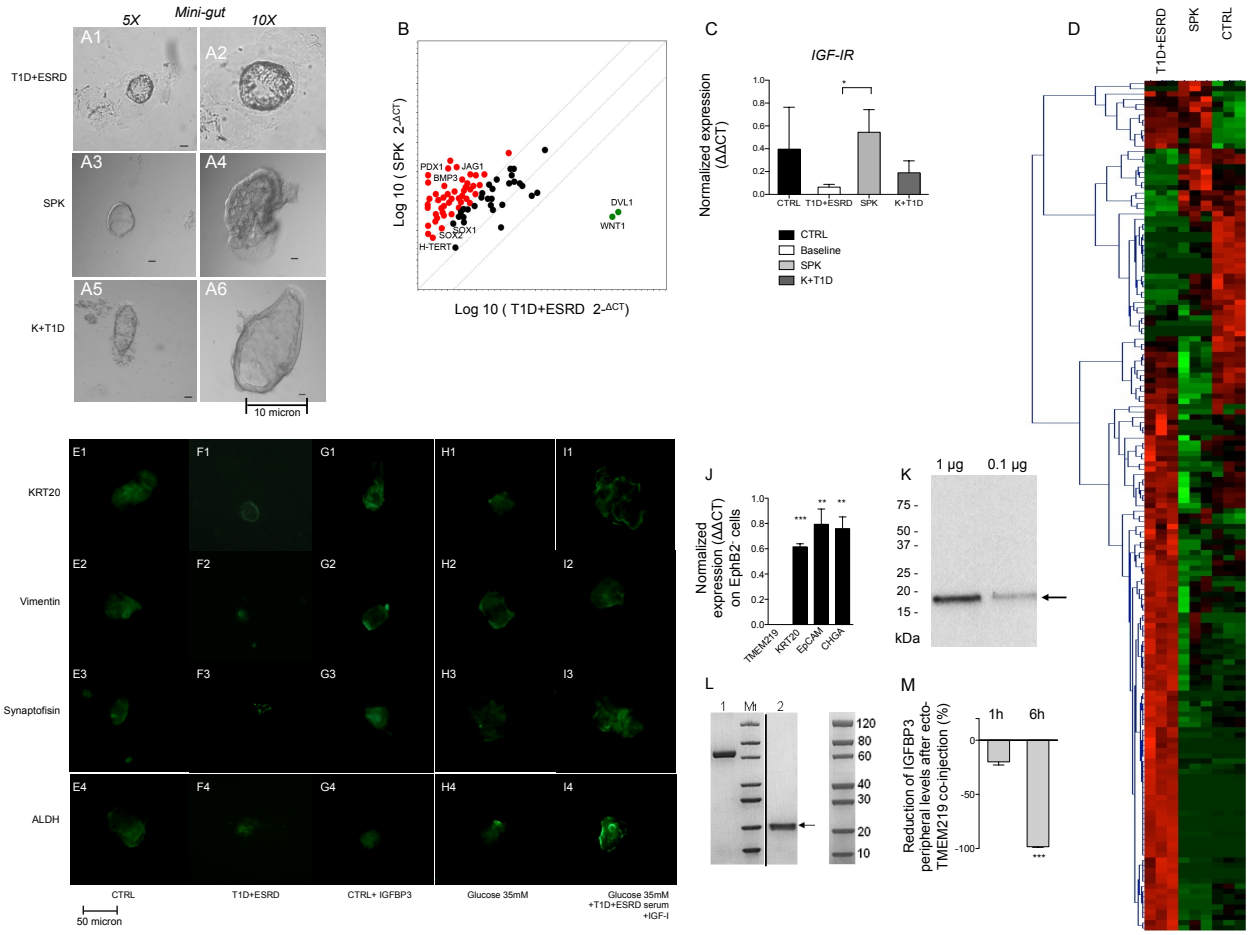

Figure S6. Analysis of colonic stem cells, IGF-IR and proteomic profile of circulating factors in diabetic enteropathy in SPK and K+T1D groups. Expression of cell lineage markers in mini-guts exposed to different culturing conditions. Confirmation analysis for generation of recombinant extracellular TMEM219 protein (ecto-TMEM219). Related to Figure 5, Figure 6 and Experimental procedures.

A1-A6. Representative images of mini-guts, cultured for 8 days *in vitro* obtained from previously isolated crypts of long-standing T1D individuals, T1D+ESRD who underwent kidney pancreas (SPK) or kidney alone (K+T1D) transplantation at 8 years of follow-up. Images are shown at 5X and 10X magnification. Scale bar 10 micron. **B**. Scatterplot representing the stem cell transcriptome profiling examined in freshly isolated intestinal crypts of SPK individuals. n=3 subjects. **C**. Bar graphs depict relative expression levels of IGF-I receptor (IGF-IR) on isolated

crypts of healthy subjects (CTRL), long-standing T1D individuals (T1D+ESRD), SPK and K+T1D measured by quantitative RT-PCR. All samples were run in triplicate and normalized to the ACTB relative expression level using the ΔΔCt method. Results are expressed as mean ± SEM. **D**. Heat map represents the proteomic profile of long-standing T1D as compared to CTRL and SPK subjects at 8 years of follow-up. The complete dataset of identified and quantified proteins was subjected to statistical analysis ($p<0.05$). Significantly differentially expressed proteins were further analyzed through hierarchical clustering. Statistics are expressed as mean ± SEM. Sera of n=10 subjects per group were evaluated. **E1-E4**, **F1-F4**, **G1-G4**, **H1-H4**, **I1-I4**. Representative images (10X magnification) of cytokeratin 20 (KRT20, epithelial cells), vimentin (mesenchymal cells), synaptofisin (enteroendocrine cells) and aldehyde Dehydrogenase (ALDH, stem cells) expression in mini-guts obtained from crypts isolated from healthy subjects, CTRL (E1-E4), and T1D+ESRD individuals (F1-F4), cultured with IGFBP3 (G1-G4), Glucose 35 mM (H1-H4), and Glucose 35 mM+long-standing T1D serum (T1D+ESRD serum)+IGF-I (I1-I4). Immunofluorescence confirmed that expression of all lineage markers is reduced in mini-guts obtained from T1D+ESRD individuals as compared to CTRL (E1-E4, F1-F4), with ALDH least expressed (F4). Decreased ALDH expression was also detected in IGFBP3-treated mini-guts (G4), while mini-guts exposed to high glucose and long-standing T1D serum and treated with IGF-I showed recovery of ALDH expression. **J**. Bar graph representing expression of TMEM219, KRT20, EpCam and CHGA on non-stem cells ($EphB2^-$ cells) measured by quantitative RT-PCR. All samples were run in triplicate and normalized to the ACTB relative expression level using the ΔΔCt method. **K**. Western blot confirmation analysis for generation of recombinant extracellular TMEM219 protein (ecto-TMEM219), using anti-TMEM219 antibody. 1 μg and 0.1μg of ecto-TMEM219 were evaluated. **L**. SDS-PAGE confirmation analysis (cropped blots) for generation of recombinant extracellular TMEM219 protein (ecto-TMEM219).

M1: PAGE-MASTER Protein Standard (GenScript). Lane 1: BSA (2 μg). Lane 2: TMEM219 extracellular domain (2 μg). **M**. The co-injection of IGFBP3 and ecto-TMEM219 in B6 mice prevented the increase of human IGFBP3 peripheral levels and implies the binding of ecto-TMEM219 with IGFBP3. Peripheral levels were assessed at 1 and 6 hours after injection. Results are expressed as mean ± SEM. All parameters examined were statistically significantly different when comparing different groups as follows: $^{*}p<0.01$, $^{**}p<0.001$, $^{***}p<0.0001$.

Abbreviations: T1D, type 1 diabetes; ESRD, end stage renal disease; CTRL, healthy subjects; SPK, simultaneous kidney-pancreas transplantation; K+T1D, kidney transplantation alone in type 1 diabetes; RT-PCR, real-time polymerase chain reaction; ACTB, beta actin; IGF-IR, insulin-like growth factor 1 receptor; SEM, standard error of mean; IGF-I, insulin-like growth factor 1; IGFBP3, insulin-like growth factor binding protein 3; IF, immunofluorescence; KRT20, cytokeratin 20, ALDH, aldehyde dehydrogenase, EpCam, epithelial cell adhesion molecule; CHGA, chromogranin A; RT-PCR, real-time polymerase chain reaction; ACTB, beta actin.

SUPPLEMENTAL TABLES

Table S1. List of up- and down-regulated stem cell target genes identified by transcriptomic profiling in CTRL vs. T1D+ESRD freshly isolated colonic crypts (at least $p < 0.05$). Related to Figure 2 and S1.

Down-regulated genes			Up-regulated genes
ACTC1	APC	CD44	DVL1
BTRC	SOX1	SOX2	WNT1
CCND2	FZD1	ADAR	
ACAN	ALPI	CD8A	
COL1A1	COL2A1	COL9A1	
BMP1	BMP2	BMP3	
CCNA2	CCNE1	CDC42	
CDK1			
CTNNA1	CXCL12	PARD6A	
CD3D	CD8B	MME	
CD4			
DLL1	HDAC2	NOTCH1	
DLL3	JAG1	NOTCH2	
DTX2	KAT2A	NUMB	
EP300			
FGF2	FGF3	FGFR1	
GDF3	ISL1	KRT15	
MSX1	MYOD1	T	
GJA1	GJB1	GJB2	
KAT8	RB1	h-TERT	
NCAM1	SIGMAR1	TUBB3	
ABCG2	ALDH1A1		
PDX1			
IGF-I			
DHH			
BGLAP			

Table S2. List of up- and down-regulated stem cell target genes identified by transcriptomic profiling in colonic crypts obtained from CTRL and from T1D+ESRD and cultured with/without IGFBP3 and IGF-I (at least $p < 0.05$). Related to Figure 3 and S3.

	Down-regulated genes	**Up-regulated genes**
CTRL+ IGF-I vs. CTRL	CD44, CDH1, COL9A1	ACAN, COL2A1, DLL1, FGF2, FGF3, GDF3, GJA1, IGF-I, ISL1, MME MSX1, NCAM1, NOTCH2 PDX1, SOX1, SOX2, h-TERT
CTRL+IGFBP3 vs. CTRL	CD8B, COL9A1, RB1, SOX1 h-TERT	ASCL2, COL2A1, DHH DLL1, DTX1, DVL1, FGF3, FGF4, FOXA2 FRAT1, GDF2, HSPA9, IGF1, KAT2A, MSX1, MYC, NEUROG2, S100B WNT1
T1D+ESRD+ IGF-I vs. T1D+ESRD	ACTC1, CD3D, CD4, COL9A1 DTX1, FGFR1	ABCG2, ADAR, BMP1, BMP2, BTRC, CDC42 CTNNA1, CXCL12, DLL1 DTX2, GDF3, HDAC2 ISL1, JAG1, NOTCH1, NOTCH2, NUMB, PARD6A, PDX1, RB1, SIGMAR1, h-TERT
T1D+ESRD+ IGFBP3 vs. T1D+ESRD	ABCG2, ALDH1A1, ALPI, CD3D, CD4, CD44, CD8A, CDC42, FGF2, FGFR1, JAG1, SIGMAR1, SOX1, TUBB3	ASCL2, KAT2A, MYC, NCAM1, NEUROG2, SOX2

Abbreviations: IGF-I, insulin-like growth factor 1; IGFBP3, insulin-like growth factor binding protein 3; CTRL, healthy subjects; T1D, type 1 diabetes; ESRD, end-stage renal disease.

Table S3. List of up- and down-regulated pro/anti-apoptotic target genes identified by transcriptomic profiling in CTRL vs. T1D+ESRD freshly isolated colonic crypts and in those cultured with IGFBP3 and IGF-I (at least $p < 0.05$). Related to Figure 3 and S3.

	Down-regulated genes	**Up-regulated genes**
T1D+ESRD vs. CTRL	BCL2, NOL3, FAS	CASP1, CASP10, CASP14, CASP5, CASP6, CASP7, CASP8, CASP9, CD27, CRADD, FADD, FASLG, HRK, TNFRSF10A, TNFRSF10B, TNFRSF11B, TNFRSF1A, TNFRSF1B, TNFRSF25, TNFRSF9, TNFSF8, TRADD, TRAF3
CTRL+ IGF-I vs. CTRL	BNIPL3	CASP14, CASP5, CD27, CRADD, FASLG, TNFRSF25 TNFSF8, TRADD
CTRL+IGFBP3 vs. CTRL	BAX, BCL2	CASP5, CASP8, CASP9, FAS TNFRSF1B, TNFSF8, TRADD TRAF3
T1D+ESRD+ IGF-I vs. T1D+ESRD	CASP1, CASP10, CASP5 CASP6, CASP7, CASP8 CASP9, CRADD, FADD TNFRSF11B, TNFRSF9 TNFSF8, TRADD, TRAF3	BCL2
T1D+ESRD+ IGFBP3 vs. T1D+ESRD	BAX, BCL2, NOL3, TNFRSF1B	CASP9, CD27

Abbreviations: IGF-I, insulin-like growth factor 1; IGFBP3, insulin-like growth factor binding protein 3; CTRL, healthy subjects; T1D, type 1 diabetes; ESRD, end-stage renal disease.

Table S4. Restoration of both normoglycemia and normal renal function in SPK is associated with stable glucose/lipid metabolism and blood pressure control over time at up to 8 years of follow-up as compared to K+T1D (data are shown at 8 years of follow-up). Related to Figure 4 and 5.

Parameters	T1D+ESRD (n=60)	SPK (n=30)	K+T1D (n=30)	P value
eGFR (ml/min/1.73m^2)	< 15	65.6±20.2*	61.8±25.2§	*,§<0.0001
HbA1c (%)	8.4±1.5	5.4±0.3*	7.5±1.4§	*<0.0001;§<0.001
EIR (UI)	37.4±2.3	0*	26.0±7.0§	*<0.0001; §0.001
TG (mg/dl)	162.5±92.7	90.4±23.0*	147.1±98.0§	*0.01; §0.04
Chol (mg/dl)	201.0±45.7	185±27.2	191.1±41.1	NS
LDL (mg/dl)	116.3±40.3	119.5±34.0	97.8±2.1	NS
HDL (mg/dl)	48.1±14.4	51.4±4.1	43.13±5.7	NS
Systolic BP	146.3±18.7	133.1±14.2*	140.1±15.7§	0.03; §0.04
Diastolic BP	83.7±8.3	79.1±9.2	78.3±9.2	NS

Abbreviations: T1D, type 1 diabetes; ESRD, end-stage renal disease; SPK, simultaneous kidney-pancreas transplantation; K+T1D, kidney transplantation alone in type 1 diabetes; eGFR, estimated glomerular filtration rate; HbA1c, glycated hemoglobin; EIR, exogenous insulin requirement; TG, tryglycerides; Chol, total cholesterol; LDL, low density lipoprotein; HDL, high density lipoprotein; BP, blood pressure; UI, International Unit; NS, not significant.

Table S5. List of proteins identified by proteomic analysis. The table reports correspondence between numbers and names of proteins detected by proteomic analysis and is shown as a heat-map in Supplementary Figure 6. Related to Figure 3 and S6.

SUPPLEMENTAL VIDEOS

Video S1. Video showing the hypothesized mechanism whereby the peripheral IGF-I/IGFBP3 axis controls colonic stem cells and the effect of ecto-TMEM219. Related to Figure 4 and 6.

SUPPLEMENTAL EXPERIMENTAL PROCEDURES

Patients and study design

60 individuals with T1D+ESRD registered on the waiting list for simultaneous pancreas-kidney transplantation (SPK) matched for (age 41 to 43 years old), gender, and duration of T1D (29.4±1.8 years) were enrolled in the study. 20 healthy subjects matched for age and gender (CTRL), with normal renal function and normal glycometabolic parameters, were studied as well. T1D+ESRD subjects were all on intensive insulin treatment at the time of enrollment in the study, while the CTRL group was not being administered any medication. All T1D+ESRD subjects were on the same treatment as antiplatelet therapy (ASA) and anti-hypertension (angiotensin-converting-enzyme inhibitors), while 40 out of 60 received statins when enrolled in the study. Subjects with clear signs of inflammatory bowel diseases as well as celiac disease were not enrolled.

T1D+ESRD individuals were followed up for 8 years (mean follow-up: 8.6±1.1 years) after receiving either SPK (n=30) or K+T1D (n=30) transplantation according to the macroscopic surgical evaluation at the time of transplantation. Individuals taking an oral anticoagulant agent were not included. SPK individuals were all insulin-independent for the entire follow-up period, whereas K+T1D individuals were on intensive subcutaneous insulin therapy. All subjects provided informed consent before study enrollment. Studies not included in the routine clinical follow-up were covered by an appropriate Institutional Review Board approval (Enteropatia-trapianto/01 Secchi/Fiorina).

Transplantation and immunosuppression

Organs for transplantation were obtained from deceased donors through the “North Italia Transplant” organ procurement consortium (NITp, Milan). After induction with ATG (thymoglobulin, IMTIX, SANGSTAT), immunosuppression was maintained using cyclosporine

(through levels between 100-250 ng/ml) or FK506 (through levels between 10-15 ng/ml), mycophenolate mofetil (500-2000 mg/day), and methylprednisolone (10 mg/day). Steroids were withdrawn within 3-6 months after transplantation. All patients included in the T1D+ESRD and SPK groups were on anti-platelet therapy (80% ASA and 20% ticlopidine) to prevent graft or fistula thrombosis. Metabolic status, renal function and blood pressure were examined during enrolment and after transplantation every 2 years thereafter. The estimate glomerular filtration rate (eGFR) was calculated using the Modification of Diet in Renal Disease (MDRD) formula *(Levey et al., 1999).*

The Gastrointestinal Symptom Rating Scale (GSRS)

Gastrointestinal symptoms were evaluated by GSRS questionnaire in healthy subjects, in long-standing T1D individuals (T1D+ESRD) and in SPK and K+T1D groups at 2, 4 and 8 years after transplantation. The Gastrointestinal Symptom Rating Scale (GSRS) is a questionnaire consisting of 15 items with a seven-graded Likert scale defined by descriptive anchors(Svedlund et al., 1988). The questionnaire was originally constructed as an interview-based rating scale designed to evaluate a wide range of gastrointestinal symptoms and was later modified to become a self-administered questionnaire. The higher the scores, the more severe the symptoms: the scale ranges from a minimum value of 1 to a maximum value of 7. If an individual's participation in the study is discontinued, the value at the last available observation will be carried forward in the analysis. The items can be grouped into five dimensions previously identified on the basis of a factor analysis: abdominal pain syndrome (three items), reflux syndrome (two items), indigestion syndrome (four items), diarrhea syndrome (three items) and constipation syndrome (three items).

Anorectal manometry

Data on anorectal manometry were already available in healthy subjects, and were compared with those obtained by performing anorectal manometry in long-standing T1D individuals

(T1D+ESRD) using a custom-designed, open-tip, 14-Fr diameter, PVC probe with seven lumens and a 4-cm latex balloon tied at the end of the probe (Bioengineering Laboratories Plc., Milan, Italy) *(Carrington et al., 2014; Remes-Troche et al., 2010)*. The sphincter length was measured after a 10-minute run-in period, anal pressure was recorded for 15 minutes in resting conditions. Subjects were then instructed to squeeze the anus as tightly as possible and for as long as possible – for at least 20 seconds. Our study evaluated the following items: Resting Tone, Contraction Tone, Reflex Response, and Urgency Response.

Pathology, immunohistochemistry and electron microscopy

Colorectal endoscopy procedure was performed in healthy subjects, in long-standing T1D individuals (T1D+ESRD) at baseline and in SPK and K+T1D groups at 2, 4, and 8 years after transplantation using a Welch Allyn optic sigmoid scope. Intestinal mucosal samples were fixed in buffered formalin (formaldehyde 4% w/v and acetate buffer 0.05 M) and routinely processed in paraffin wax. 3μm-thick sections of each enrolled case were stained with Hematoxylin & Eosin (H&E) for morphological evaluations. For immunohistochemistry, 3μm-thick sections were mounted on poly-L-lysine coated slides, deparaffinized and hydrated through graded alcohols to water. After antigen retrieval, performed by dipping sections in 0.01 M citrate buffer, pH 6 for 10 minutes in a microwave oven at 650W as well as endogenous peroxidase activity inhibition, performed by dipping sections in 3% hydrogen peroxide for 10 minutes, incubation with primary antibodies was performed at 4°C for 18–20 hours, followed by the avidin-biotin complex procedure *(Hsu et al., 1981)*. Immunoreactions were developed using 0.03% 3,3'diaminobenzidine tetrahydrochloride, and then sections were counterstained with Harris' hematoxylin. The following antibodies were used: Ki67 (monoclonal, clone MIB1, 1:100 dilution, Dako, Carpinteria, CA, USA), aldehyde dehydrogenase (monoclonal, clone 44/ALDH, 1:1000 dilution, Transduction Laboratories, Franklin Lakes, NJ, USA), EphB2 (monoclonal,

clone 48CT12.6.4, 1:200 dilution, Lifespan Biosciences, Seattle, WA, USA), LGR5 (monoclonal, clone 2A2, 1:100 dilution, Origene Technologies, Rockville, MD, USA), hTERT (monoclonal, clone Y182, 1:500 dilution, Millipore, Billerica, MA, USA), glicentin (polyclonal, 1:1250 dilution, Milab, Malmo, Sweden), pancreatic polypeptide (polyclonal, 1:500 dilution, Peninsula, Belmont, CA, USA), PYY (polyclonal, 1:1000 dilution, Biogenesis, Bournemouth, UK), serotonin (monoclonal, clone YC5, 1:50 dilution, Biogenesis), somatostatin (polyclonal, 1:550 dilution, Dako), IGF-I (polyclonal, 1:500, Abcam) and IGF-IR (polyclonal, 1:100, Cell Signaling Technologies), *(Fiorina et al., 2003)*. For ultrastructural studies, samples were fixed for 2 hours at 4°C in a mixture of 2% paraformaldehyde and 2% glutaraldehyde in 0.05 M cacodylate buffer, pH 7.3. They were post-fixed in 1% osmium tetroxide for 1 hour at room temperature, then dehydrated and embedded in Epon-Araldite. Ultrathin sections were cut with a diamond knife and mounted on 200-mesh nickel grids, previously coated with a Formvar film. Ultrathin sections were stained with aqueous uranyl acetate and Reynold's lead citrate solutions and subsequently examined with a Philips Morgagni 268D electron microscope. Cases were grouped according to the number of neuroendocrine vesicles ($n > 3$ and $n < 3$) for statistical analysis. For crypt isolation, tissue was collected in a sample containing a mixture of antibiotics and processed as described in the next paragraph. The immunostaining intensity for EphB2 was graded as 1 (negative EphB2 gradient to few cells positive per crypt per field) to 5 (strong EphB2 gradient in all longitudinal crypts). An anti-IGFBP3 primary antibody (polyclonal, 1:50 dilution, Sigma Aldrich) was immunohistochemically tested in liver biopsies from patients with type 1 diabetes. Liver biopsies without pathological findings were used as controls. All of these tissue samples came from the files stored at the Unit of Pathology of the Department of Biomedical, Biotechnological, and Translational Sciences, University of Parma, Parma, Italy. The

immunostaining intensity was graded as 1 (mild), 2 (moderate), and 3 (strong), while its diffusion as 1 (focal), 2 (zonal), and 3 (diffuse).

Immunoflurescence

Immunofluorescence samples obtained from liver biopsies were observed using a confocal system (LSM 510 Meta scan head integrated with the Axiovert 200 M inverted microscope; Carl Zeiss, Jena, Germany) with a 63x oil objective. Images were acquired in multitrack mode, using consecutive and independent optical pathways. The following primary antibodies were used: rabbit IGFBP3 (1:10, Sigma) mouse Hep Par-1 (1:20, monoclonal, Dako), mouse CD163 (1:10, cloneMRQ26, CellMarque).

Mini-guts co-cultured with/without IGFBP3, with/without long-standing T1D serum + high glucose (35 mM Glucose) and those obtained from crypts of long-standing T1D individuals, were stained with vimentin, cytokeratin 20, aldheide dehydrogenase and synaptofisin for immunofluorescence analysis to assess expression of cell lineage markers (Fig. S6: E1-E4, F1-F4, G1-G4, H1-H4, I1-I4). The following primary antibodies were used: mouse vimentin (1:80, monoclonal, clone V9 Dako) mouse aldheyde (1:1000, monoclonal, clone 44, BD), mouse cytokerain 20 (1:100, monoclonal, clone Ks20.8, Dako) and synaptofisin (1:100, monoclonal, clone syn88, BioGenex).

CoSC characterization

Crypt purification

Muscle layer and sub-mucosa were carefully removed from human fresh rectal biopsy specimens, and mucosa was incubated with a mixture of antibiotics (Normocin, [Invivogen, San Diego, California 92121, USA], Gentamycin [Invitrogen, Carlsbad, CA,USA] and Fungizone [Invitrogen]) for 15 minutes at room temperature (RT). Next, tissue was cut into small pieces and incubated with 10 mM Dithiotreitol (DTT) (Sigma, St. Louis, MO 63103, USA) in PBS 2-3 times

for 5 minutes at RT. Samples were then transferred to 8 mM EDTA in PBS and slowly rotated for 60-75 minutes at 4°C. Supernatant was replaced by fresh PBS, and vigorous shaking of the sample yielded supernatants enriched in colonic crypts. Fetal bovine serum (FBS, Sigma) was added to a final concentration of 5%, and fractions were centrifuged at 40×g for 2 minutes in order to remove single cells. This washing procedure was repeated 3 times with Advanced DMEM/F12 (ADF, Gibco) medium supplemented with 2 mM GlutaMax (Invitrogen), 10 mM HEPES (Sigma), and 5% FBS (Sigma).

200-300 isolated human colonic crypt units were mixed with 50 µl matrigel and plated on pre-warmed 24-well culture dishes as already described. After solidification (15-20 minutes at 37°C), crypts were overlaid with 600 µl complete crypt culture medium [Wnt3a-conditioned medium and Advanced DMEM/F12 (Life Technologies, Grand Island, NY) 50:50, supplemented with Glutamax, 10 mM HEPES, N-2 [1×], B-27 without retinoic acid [1×], 10 mM Nicotinamide, 1 mM N-Acetyl-L-cysteine, 50 ng/ml human EGF (Life Technologies, Grand Island, NY), 1 µg/ml RSPO1 (Sino Biological, Beijing, China), 100 ng/ml human Noggin (Peprotech, Rocky Hill, NJ, USA), 1 µg/ml Gastrin (Sigma-Aldrich, St. Louis, MO), 500 nM LY2157299 (Axon MedChem, Groningen, The Netherlands), 10 µM SB202190 (Sigma) and 0.01 µM PGE2 (Sigma)]. Medium was replaced every other day. Rock inhibitor Y-27632 (10 µM, Sigma) was added to the cultures for the first 2-3 days. Purified crypts were directly cultured for 8 days. Cell lineage markers for enterocytes and enteroendocrine cells were assessed in mini-guts and in the $EphB2^{+}$ and $EphB2^{-}$ sorted single cells with RT-PCR by examining: CHGA, KRT20 and EPCAM (Life Technologies, Grand Island, NY). Colony forming efficiency (%) was evaluated on freshly isolated crypts in order to exclude that the bioptic procedure and the isolation processing could have compromized their efficiency in forming mini-guts in *in vitro* culture. DAPI staining was performed to confirm number of nuclei in freshly isolated crypts from CTRL and T1D+ESRD subjects. Developed

mini-guts with at least 1 crypt domain were also counted, and their percentage was calculated in order to use more quantitative criteria to measure developed mini-guts (data not shown). Insulin and glucose levels measured on long-standing T1D (T1D+ESRD) and CTRL serum are reported below:

Glucose levels (T1D+ESRD vs. CTRL, 178±47.5 vs 90±5.5 mg/dl, p=0.0001);

Insulin levels (T1D+ESRD vs. CTRL, 12.9±4.6 vs 5.8±1.6 μIU/ml, p=0.009).

Flow cytometry

The expression of the CoSC markers EphB2 (APC anti-human EphB2 antibody, R&D, Minneapolis, MN) and LGR5 (PE anti-human LGR5, Origene, Rockville, MD) was determined by flow cytometry by excluding CD45- and CD11b-positive cells (V450 anti-human CD45 and CD11b, BD Biosciences, San Jose, CA). Propidium iodide (PI) was added (10 μg/ml) to exclude dead cells. $EphB2^{+}$ cells were also sorted by flow cytometry to obtain a single cell suspension for culturing purposes. Intracellular detection of human-tert (hTERT) was performed by permeabilizing cells and staining with primary anti-human hTERT antibody (GeneTex, Irvine, CA) followed by DAPI anti-goat secondary antibody (Life Technologies). With regard to the analysis, cells were all first gated as PI^{-} before the assessment of other surface or intracellular markers. Samples were run on a BD LSR-Fortessa and analyzed by FSC Express 3.0 (DeNovo Software, Los Angeles, CA, USA).

In vitro mini-gut generation study

Crypts were isolated from healthy subject rectal biopsy samples and cultured as previously described to generate mini-guts. To create hyperglycemic conditions, the culturing medium was modified by adding glucose at different concentrations (35 mM: high glucose; 5 mM: normal glucose). To mimic uremic conditions, human uremic serum obtained from long-standing T1D individuals with ESRD was added to crypts, which were cultured as reported in the crypt

culturing methods section. After 8 days, crypts were collected, and the morphology, mini-gut growth, expression of intestinal signature markers (EphB2, LGR5, h-TERT), IGF-IR and TMEM219 (transmembrane protein 219, Life Technologies), and Caspase 9 (Life Technologies) were examined using RT-PCR. A pan-caspase inhibitor (caspase inhibitor Z-VAD-FMK, 20 mM, Promega, Madison, WI), a Caspase 8-selective inhibitor (Z-IETD-FMK, BD Pharmingen), a Caspase 9-selective inhibitor (Z-LEHD-FMK, BD Pharmingen), and a Caspase 3 inhibitor (Z-DEVD-FMK, BD Pharmingen) were used *in vitro* in mini-guts to confirm the anti-apoptotic effect of IGFBP3.

To culture isolated crypts with crypt culturing medium containing healthy subject human serum, namely "CTRL" serum, in place of regular FBS, L-Wnt3 cells were grown in 10% "CTRL" serum to generate conditioned medium that was further added 50:50 to Advanced DMEM/F12 medium in order to obtain the crypts culture medium as described above (see *Crypt purification*).

To assess the properties of sorted EphB2$^+$ cells in generating mini-guts, 2000 sorted cells were mixed with 50 µl matrigel and plated on pre-warmed 24-well culture dishes. After solidification of the matrigel (10-15 min at 37°C), cells were overlaid with "single cell growth medium" (= complete crypt culture medium+10 M Rock inhibitor Y-27623). Medium was replaced with fresh single cell growth medium every other day. Rock inhibitor was included in the culture medium for 7-9 days.

Immunoblotting

Total proteins of intestinal bioptic samples were extracted in Laemmli buffer (Tris–HCl 62.5 mmol/l, pH 6.8, 20% glycerol, 2% SDS, 5% β-mercaptoethanol) and their concentration was measured *(Lowry et al., 1951)*. 35 µg of total protein was electrophoresed on 7% SDS-PAGE gels and blotted onto nitrocellulose (Schleicher & Schuell, Dassel, Germany). Blots were then stained with Ponceau S. Membranes were blocked for 1 h in TBS (Tris [10 mmol/l], NaCl [150mmol/l]),

0.1% Tween-20, 5% non-fat dry milk, pH 7.4 at 25° C, incubated for 12 h with 200 mg/ml of a polyclonal anti-goat EphB2 antibody or polyclonal anti-goat LGR5 antibody (Santa Cruz Biotechnology, Santa Cruz, CA, USA) or monoclonal IGF-IR (Santa Cruz Biotechnology) and polyclonal TMEM219 (R&D, Minneapolis, MN) diluted 1:200 or with a monoclonal mouse anti-β-actin antibody (Santa Cruz Biotechnology) diluted 1:1000 in TBS–5% milk at 4° C, washed four times with TBS–0.1% Tween-20, then incubated with a peroxidase-labeled rabbit anti-goat IgG secondary antibody (or rabbit anti mouse for β-actin) diluted 1:1000 (Santa Cruz Biotechnology) in TBS–5% milk, and finally washed with TBS–0.1% Tween-20. The resulting bands were visualized using enhanced chemiluminescence (SuperSignal; Pierce, Rockford, IL, USA).

In situ hybridization

Paraffin sections of human colon mucosa were de-paraffinized and re-hydrated according to standard procedures. After treatment of sections using 0.2M HCl for 15 minutes at room temperature, sections were washed 3 times in PBS and incubated for 15 min at 37ºC in proteinase K (30 µg/ml in PBS). 0.2% glycine in PBS was added for 1 minute in order to neutralize Proteinase K activity, and samples were washed twice in PBS. After post-fixation in 4% PFA for 10 min at room temperature and 3 washes in PBS, histone acetylation was achieved by incubating samples two times for 5 min in an aqueous solution containing 1.5% triethanolamine, 0.15% HCl, and 0.6% acetic anhydride. Samples were then washed and pre-hybridized for 1 hour at 68ºC in hybridization solution (50% formamide, 5X SSC, pH4.5, 2% Blocking Reagent (Roche), 0.05% CHAPS (Sigma), 5mM EDTA, 50 µg /ml Heparin (Sigma) and 50 µg/ml yeast RNA. For TMEM219, the digoxigenin-labelled probe was diluted 750 ng/ml in hybridization solution and incubated for 24 hrs at 65ºC. Post-hybridization washes were performed 3X 20 min in 50% Formamide / 2XSSC at 65ºC. Sections were rinsed in TBS-T buffer (0.1M TrisHCl pH7.5,

0.15M NaCl, 0.1% Tween20) and blocked for 30 min at room temperature in Blocking Solution (0.5% Blocking Reagent, 10% sheep serum in TBS-T). Sheep anti-DIG antibody (Fab fragment, Roche) was diluted 1/2000 in Blocking Solution and incubated overnight at 4ºC. After this, samples were washed in TBS-T and then in NTM buffer (0.1M Tris pH9.5, 0.1M NaCl, 0.05M MgCl2) and developed in NBT/BCIP solution (Roche) for 24 hrs.

Morphology imaging analysis

The images of mini-guts were taken at day 0, 5 and 8 days by inverted microscopy Leica DH/RB and acquired with Axio Vision AC Release 4.3. Pictures reported in figures represent mini-guts at day 5, 10X magnification.

Transcriptome profiling

Total RNA was isolated from purified intestinal crypt suspension using the RNeasy Mini Kit (Qiagen, Valencia, CA) with on-column DNase I digestion. Next, 3 µg total RNA from each sample was reverse-transcribed using the RT2 First Strand kit (C-03; SABiosciences, Frederick, MD). We used the Human Stem Cell RT2 Profiler PCR Arrays (PAHS-405Z), the human Stem Cell Signaling PCR Array (PAHS-047Z,) and a custom array with the following genes: AXIN2, OLFM4, BMI1, RNF43, CDCA7, SLC12A2, CDK6, SOX9, DKC1, ZNRF3, ETS2, EPHB2, FAM84A, LGR5, GPX2, ACTB (SABiosciences). The Profiler PCR Arrays measure quantitatively the expression of a panel of genes using SYBR Green-based real-time PCR (Kosinski et al., 2007). To assess the transcriptome profile of apoptotic markers and oxidative stress markers, Human Apoptosis PCR Arrays (PAHS-012Z, SABiosciences) and Human Oxidative Stress PCR Arrays (PAHS-065Z, SABiosciences) were used.

qRT-PCR analysis

RNA from purified intestinal crypts was extracted using Trizol Reagent (Invitrogen), and qRT-PCR analysis was performed using TaqMan assays (Life Technologies, Grand Island, NY)

according to the manufacturer's instructions. The normalized expression values were determined using the ΔΔCt method. Quantitative reverse transcriptase polymerase chain reaction (qRT-PCR) data were normalized for the expression of ACTB, and ΔΔCt values were calculated. Statistical analysis compared gene expression across all cell populations for each patient via one-way ANOVA followed by Bonferroni post-test for multiple comparisons between the population of interest and all other populations. Statistical analysis was performed also by using the software available RT^2 profiler PCR Array Data Analysis (Qiagen). For two groups comparison Student *t* test was employed. Analysis was performed in triplicates after isolation of fresh crypts and/or after 8 days of culture of miniguts. Below are reported the main characteristics of primers used:

Gene Symbol	UniGene #	Refseq Accession #	Band Size (bp)	Reference Position
LGR5	Hs.658889	NM_003667	91	1665
EPHB2	Hs.523329	NM_004442	68	2908
TERT	Hs.492203	NM_198253	106	1072
ACTB	Hs.520640	NM_001101	174	730
IGF-IR	Hs.643120	NM_000875.3	64	2248
TMEM219	Hs.460574	NM_001083613.1	60	726
KRT20	Hs.84905	NM_019010.2	75	974
CHGA	Hs.150793	NM_001275.3	115	521
EpCam	Hs.542050	NM_002354.2	95	784
LRP1	Hs.162757	NM_002332.2	64	656
TGFbR1	Hs.494622	NM_001130916.1	73	646
TGFbR2	Hs.604277	NM_001024847.2	70	1981
Caspase 8	Hs.599762	NM_001080124.1	124	648
Caspase 9	Hs.329502	NM_001229.4	143	1405
CTNNB1	Hs.476018	NM_001098209.1	67	2048

ELISA assay

IGF-I and IGFBP3 levels in the pooled sera/plasma of all groups of subjects and in all groups of treated and untreated mice were assessed using commercially available ELISA kits, according to the manufacturer's instructions (R&D and Sigma).

The human immortalized hepatoma cell line HuH-7 was cultured for 5 days in DMEM 10% FBS at different glucose concentrations: 5.5 mM, 20 mM and 35.5 mM. Culturing supernatant was collected, and IGFBP3 was assessed using an IGFBP3 ELISA kit (Sigma) according to the manufacturer's instructions. Collected cells were separated by trypsin and counted with a hemacytometer.

Insulin levels were assayed with a microparticle enzyme immunoassay (Mercodia Iso-Insulin ELISA) with intra- and inter-assay coefficients of variation (CVs) of 3.0% and 5.0%.

Recombinant proteins and interventional studies

Recombinant human IGF-I (Sigma, I3769), (IGF-I), recombinant human IGFBP3 (Life Technologies, 10430H07H5), (IGFBP3), and anti-IGF-IR (Selleckchem, Boston, OSI-906) were added to crypt cultures at day +2 from isolation. IGFBP3 (Reprokine, Valley Cottage, NY) was administered to naive and to STZ-treated B6 mice at 150 μg /mouse/day for 15 days intraperitoneally (i.p.); IGF-I (Reprokine) and ecto-TMEM219 were administered in vivo to STZ-treated B6 mice intraperitoneally (i.p.) after 2 weeks of diabetes at a dose of 5 μg/mouse/day for 20 days and 100 μg/mouse/day for 15 days, respectively.

Other molecules tested in our *in vitro* mini-guts assay and added to crypt cultures at day +2 from isolation: adiponectin (R&D), thymosin β4 (Abcam), C-reactive protein (Merck Millipore), cystatin C (Cell Signaling Technologies), chromogranin A (Life Technologies), fructose-bisphosphate aldolase (Novoprotein), osteopontin (R&D), pancreatic ribonuclease (RNASE, Novoprotein), serum amyloid A protein (Abcam), mannan-binding lectin serine protease 1 (MASP1, Novoprotein), tumor necrosis factor-alpha (TNF-alpha, R&D), Fas ligand (FasL, R&D) and hydrogen peroxide (H2O2, 50 μM).

Generation of ecto-TMEM219 recombinant protein

Recombinant human ecto-TMEM219 was generated using *E. coli* for expression for synthesis. The amino acid sequence of extracellular TMEM219 that was used was as follows:

THRTGLRSPDIPQDWVSFLRSFGQLTLCPRNGTVTGKWRGSHVVGLLTTLNFGDGPDRN KTRTFQATVLGSQMGLKGSSAGQLVLITARVTTERTAGTCLYFSAVPGILPSSQPPISCSE EGAGNATLSPRMGEECVSVWSHEGLVLTKLLTSEELALCGSR.

The DNA sequence of extracellular TMEM219 was cloned into a high-copy number plasmid containing the lac promoter, which was then transformed into *E. coli*. Addition of IPTG induced the bacteria to express extracellular TMEM219 (ecto-TMEM219). SDS-PAGE and western Blot were used to confirm purity higher than 90%. The molecular weight of the new generated recombinant protein human ecto -TMEM219 was 18.2 kDa (GenScript Inc. Piscataway, NJ, USA).

Crypts from healthy subjects were isolated and cultured as previously described and ecto-TMEM219 was added to the culture at three concentrations (260 ng/ml, 130 ng/ml and 75 ng/ml) as compared to IGFBP3 concentration used (2:1, 1:1 and 1:2), and appropriate controls were employed for each concentration. After 8 days of culture, expression of Caspases 8 and 9, of CoSC signature markers (EphB2 and LGR5), and number of developed mini-guts were further assessed.

Small RNA interference

Isolated crypts obtained from healthy subjects were grown to generate *in vitro* mini-guts in complete medium and in culturing medium modified by adding high glucose and long-standing T1D serum as previously described (see i*n vitro mini-gut generation study* in online methods). After 72h of culture, which allowed the crypts to recover, 750 ng of small interfering RNA (siRNA; Flexitube siRNA SI04381013, Qiagen, Valencia, CA) in 100 µl culture medium without serum and with 6 µl HiPerFect Transfection Reagent (Qiagen) were incubated at room

temperature to allow for the formation of transfection complexes. Crypts were incubated with these transfection complexes under their normal growth conditions for 6h. Analysis of gene silencing was performed at 24, 48 and 72h by evaluating the percentage of normal mini-gut development. Control siRNA was used as a negative control to confirm the effect of gene silencing.

Proteomic analysis

8 µl of pooled serum from 10 patients per group were depleted using a ProteoPrep 20 spin column (Sigma), thus allowing for the removal of the 20 highly abundant proteins. The procedure was twice repeated in order to obtain ~99% depletion, according to the manufacturer's instructions. The recovered supernatant was analyzed to determine total protein concentration using the Direct Detect IR spectrophotometer and BSA as a standard. In order to obtain enough protein for proteomic analysis, 32 µl from each pool were processed as above described. 40 µg of total protein from each sample was in-solution digested using the Filter Aided Sample Preparation (FASP) protocol as reported in the literature *(Wisniewski et al., 2009)*. Samples were desalted using C18 homemade tip columns (C18 Empore membrane, 3M) and injected into a capillary chromatographic system (EasyLC, Proxeon Biosystems, Thermo Scientific). Peptide separations were performed on a homemade 25 cm reverse phase spraying fused silica capillary column, packed with 3 µm ReproSil Pur 120 C18-AQ. A gradient of eluents A (pure water with 2% v/v ACN, 0.5% v/v acetic acid) and B (ACN with 20% v/v pure water with 0.5% v/v acetic acid) was used to achieve separation (0.15 µL/minute flow rate) (from 10 to 35% B in 230 minutes, from 35 to 50% B in 5 minutes and from 50 to 70% B in 30 minutes). Mass spectrometry analysis was performed using an LTQ-Orbitrap mass spectrometer (Thermo Scientific, Waltham, MA) equipped with a nanoelectrospray ion source (Proxeon Biosystems). Full scan mass spectra were acquired with the lock-mass option and resolution set to 60,000. The

acquisition mass range for each sample was from *m*/*z* 300 to 1750 Da. The ten most intense doubly and triply charged ions were selected and fragmented in the ion trap using a normalized collision energy 37%. Target ions already selected for the MS/MS were dynamically excluded for 120 seconds. All MS/MS samples were analyzed using Mascot (v.2.2.07, Matrix Science, London, UK) search engine to search the UniProt_Human Complete Proteome_ cp_hum_2013_12. Searches were performed with trypsin specificity, two missed cleavages allowed, cysteine carbamidomethylation as fixed modification, acetylation at protein N-terminus, and oxidation of methionine as variable modification. Mass tolerance was set to 5 ppm and 0.6 Da for precursor and fragment ions, respectively. To quantify proteins, the raw data were loaded into the MaxQuant software version 1.3.0.5 *(Cox et al., 2011)*. Label-free protein quantification was based on the intensities of precursors. Peptides and proteins were accepted with an FDR less than 1%, two minimum peptides per protein. The experiments were performed in technical triplicates. The complete dataset of proteins, obtained by proteomic analysis (Table S5), was analyzed by Student's t-test using MeV software v. 4_8_1. 47 proteins, which were significantly different (p-value <0.01) in control pool *versus* T1D-ESDR pool, were further submitted to hierarchical clustering analysis.

Strategy to select candidate proteins

Among the 46 factors that segregated separately in long-standing T1D subjects and healthy controls, we first selected those with a more significant difference in LFQ intensity in comparing the two groups (p>0.005), leading to the exclusion of 12 factors. Next, we evaluated whether altered factors may be associated with intestinal disorders and/or with the development of diabetes by searching for existing studies and publications in the field. This led us to exclude another 12 factors. We also excluded those factors primarily related to the lymphoid compartment (n=5). This then left 17 factors. We excluded cell membrane proteins (n=4) and

proceeded with testing the remaining (n=13) in the mini-gut assay. Two factors were not available to be tested in vitro. We therefore tested n=11 proteins in total.

Animal studies

C57BL/6 (B6) mice were obtained from the Jackson Laboratory, Bar Harbor, Maine. All mice were cared for and used in accordance with institutional guidelines approved by the Harvard Medical School Institutional Animal Care and Use Committee. Mice were rendered diabetic with streptozotocin injection (225 mg/kg, administered i.p.; Sigma). Diabetes was defined as blood glucose levels >250 mg/dL for 3 consecutive measures. Diabetic enteropathy was assessed as follows: briefly, the entire intestine was extracted from sacrificed mice and flushed with PBS. The extreme part of the colon was then cut and divided in two pieces. One piece of colon tissue was directly submerged in formalin while the other was cut longitudinally to expose the lumen and the internal mucosa and then submerged in formalin. Tissue was then paraffin embedded and processed for H&E and immunostaining. In addition, colonic tissue was also cut, and isolation of colonic stem cells was performed as previously described (Merlos-Suarez et al., 2011). Briefly, colon was cut into 2–4 mm pieces, and the fragments were washed in 30 mL ice-cold PBS. Fragments were the transferred in 50 ml tubes containing pre-warmed 20 mM EDTA-PBS and incubated at 37°C for 30 min. After incubation the suspended tissue was transferred into tube containing 30 ml cold PBS and centrifuged. Crypts were resuspended in 13 ml cold DMEMF12, washed with PBS and digested in 5-10 ml of trypsin/DNase solution at 37°C for 30 min. Crypts were then resuspended in DMEMF12/EDTA, filtered through a 40-micron strainer twice, and washed. Finally, crypts were then resuspended in flow medium (DMEM+FBS+EDTA) and stained for anti EphB2 APC (R&D), mouse anti-CD45 PerCP and mouse anti-CD11b PE (BD Pharmingen). Samples were run using a FACSCalibur Analyzer and data analyzed with FlowJo.

A portion of the tissue was also snap-frozen and stored in Trizol to perform RT-PCR studies for the following markers:

Gene Symbol:	**UniGene #:**	**Refseq Accession #:**	**Band Size (bp)**:	**Reference Position**:
LGR5	Mm.42103	NM_010195.2	64	571
EPHB2	Mm.250981	NM_010142.2	85	1696
Casp8	Mm.336851	NM_001080126.1	96	1525
Casp9	Mm.88829	NM_001277932.1	68	377
GAPDH	Mm. 304088	NM_008084.2	107	75

Finally, plasma and serum were collected to perform analysis of IGF-I (IGF-I ELISA kit, R&D), IGFBP3 (IGFBP3 ELISA kit, R&D) and insulin levels (Mouse Insulin ELISA kit, Mercodia). Blood glucose was monitored twice per week for 8 weeks in order to confirm diabetes onset and permanence.

Statistical analysis

Data are presented as mean and standard error of the mean (SEM) and were tested for normal distribution with the Kolmogorov-Smirnov test and for homogeneity of variances with Levene's test. The statistical significance of differences was tested with two-tailed *t*-test and the chi-square ($\chi 2$) tests. Significance between the two groups was determined by two-tailed unpaired Student's *t* test. For multiple comparisons, the ANOVA test with Bonferroni correction was employed. All data were entered into Statistical Package for the Social Science (SPSS®, IBM®, SPSS Inc., Chicago, IL) and analyzed. Graphs were generated using GraphPad Prism version 5.0 (GraphPad Software, La Jolla, CA). All statistical tests were performed at the 5% significance level.

SUPPLEMENTAL REFERENCES

Levey, A.S., Bosch, J.P., Lewis, J.B., Greene, T., Rogers, N., and Roth, D. (1999). A more accurate method to estimate glomerular filtration rate from serum creatinine: a new prediction equation. Modification of Diet in Renal Disease Study Group. Annals of internal medicine *130*, 461-470.

Svedlund, J., Sjodin, I., and Dotevall, G. (1988). GSRS--a clinical rating scale for gastrointestinal symptoms in patients with irritable bowel syndrome and peptic ulcer disease. Digestive diseases and sciences *33*, 129-134.

Carrington, E.V., Brokjaer, A., Craven, H., Zarate, N., Horrocks, E.J., Palit, S., Jackson, W., Duthie, G.S., Knowles, C.H., Lunniss, P.J., et al. (2014). Traditional measures of normal anal sphincter function using high-resolution anorectal manometry (HRAM) in 115 healthy volunteers. Neurogastroenterology and motility : the official journal of the European Gastrointestinal Motility Society.

Remes-Troche, J.M., De-Ocampo, S., Valestin, J., and Rao, S.S. (2010). Rectoanal reflexes and sensorimotor response in rectal hyposensitivity. Diseases of the colon and rectum *53*, 1047-1054.

Hsu, S.M., Raine, L., and Fanger, H. (1981). Use of avidin-biotin-peroxidase complex (ABC) in immunoperoxidase techniques: a comparison between ABC and unlabeled antibody (PAP) procedures. The journal of histochemistry and cytochemistry : official journal of the Histochemistry Society *29*, 577-580.

Fiorina, P., Folli, F., Bertuzzi, F., Maffi, P., Finzi, G., Venturini, M., Socci, C., Davalli, A., Orsenigo, E., Monti, L., et al. (2003). Long-term beneficial effect of islet transplantation on diabetic macro-/microangiopathy in type 1 diabetic kidney-transplanted patients. Diabetes care *26*, 1129-1136.

Lowry, O.H., Rosebrough, N.J., Farr, A.L., and Randall, R.J. (1951). Protein measurement with the Folin phenol reagent. The Journal of biological chemistry *193*, 265-275.

Kosinski, C., Li, V.S., Chan, A.S., Zhang, J., Ho, C., Tsui, W.Y., Chan, T.L., Mifflin, R.C., Powell, D.W., Yuen, S.T., et al. (2007). Gene expression patterns of human colon tops and basal crypts and BMP antagonists as intestinal stem cell niche factors. Proceedings of the National Academy of Sciences of the United States of America *104*, 15418-15423.

Wisniewski, J.R., Zougman, A., Nagaraj, N., and Mann, M. (2009). Universal sample preparation method for proteome analysis. Nature methods *6*, 359-362.

Cox, J., Neuhauser, N., Michalski, A., Scheltema, R.A., Olsen, J.V., and Mann, M. (2011). Andromeda: a peptide search engine integrated into the MaxQuant environment. Journal of proteome research *10*, 1794-1805.

Merlos-Suarez, A., Barriga, F.M., Jung, P., Iglesias, M., Cespedes, M.V., Rossell, D., Sevillano, M., Hernando-Momblona, X., da Silva-Diz, V., Munoz, P., et al. (2011). The intestinal stem cell signature identifies colorectal cancer stem cells and predicts disease relapse. Cell Stem Cell *8*, 511-524.